Journal of Machine Engineering, 2024, Vol. 24
ISSN 1895-7595 (Print) ISSN 2391-8071 (Online)

Received: 09 November 2024 / Accepted: 26 November 2024 / Published online: *28 November 2024*

parallel robots, dynamics,
Gough-Stewart platform,
PD and forces compensation controller

Ha Huy HUNG[1,*], Phan Bui KHOI[2],
Hoang Quang CHINH[1], Dinh Quan NGUYEN[1],
Ha Thanh HAI[3]

DYNAMIC MODEL AND PD CONTROL WITH FORCES COMPENSATION OF DUAL-STAGE GOUGH-STEWART PLATFORM

This paper investigates a dual-stage Gough-Stewart platform. The lower platform is responsible for simulating the oscillations of moving vehicles such as cars, ships, and airplanes. The upper platform is connected to devices that require either balance stabilization or motion stabilization according to specific requirements. The dynamic model of the robot system is derived in a general form based on the Lagrange equations of motion with Lagrange multipliers. Using these equations in a compact form, a PD controller with forces compensation in task space is designed for the robot system. Oscillation generation and balance stabilization are computed and simulated using the kinematic and dynamic parameters of two Bosch Rexroth robots. The computation and simulation results demonstrate the dynamic model's accuracy and the controller's effectiveness.

1. INTRODUCTION

The robot system comprises two Gough-Stewart platforms (GSP) [1], positioned in lower and upper stages. Each GSP has an upper work plate and a lower base plate, connected by six legs with universal joints. The leg lengths on both platforms are adjusted using either electric motors or hydraulic cylinders. Figure 1 shows the dual-stage Gough-Stewart platform, with the lower stage generating oscillations and the upper stage maintaining stability. The sensors are attached to the work plates of both stages to directly measure the position, orientation, velocity, and angular velocity of these plates.

The GSP has a high rigid structure and accurate positioning, making it applicable in various fields such as flight simulation, robotic surgery, mobile stabilization platforms, precision machining, vibration compensation in machining (functions like the hybrid six sigma mechanism [2]). Many devices on transportation vehicles, such as cars, ships, and

[1] Department of Mechatronics, Faculty of Aerospace Engineering, Le Quy Don Technical University, Vietnam
[2] School of Mechanical Engineering, Hanoi University of Science and Technology, Hanoi, Vietnam
3 Faculty of Industrial & Systems engineering, Hanoi University of Industry, Vietnam
[*] E-mail: hahuyhung@lqdtu.edu.vn
https://doi.org/ 10.36897/jme/196504

aircraft, require balance stabilization for items like cooking tables, treatment tables, and gangways between ships and offshore rigs [3,4]. The GSP is used to regenerate the oscillations of moving vehicles, creating a semi-natural simulation system for balance stabilization control. This approach addresses the high cost, time demands, and complexity of conducting stability control research directly on actual mobile platforms across various vehicle types and terrains.

Numerous studies have focused on dynamics modeling and control of GSPs, employing motion equations such as Newton-Euler, Lagrange, Kane, or virtual work principles [5-7]. Control strategies for GSPs include kinematic control, inverse dynamics control in joint or task space, PID, sliding mode, and adaptive controls, etc [8-10]. However, while single-stage GSP is commonly explored, studies on multi-stage GSPs are less common due to the complexity of its closed-chain structure and high degrees of freedom [9-14].

This paper presents a dynamic model and PD control with forces compensation in task space for dual-stage GSP, using a multibody approach with Lagrange's equations and multipliers. The paper is organized as follows: Section 1 introduces the study; Section 2 derives kinematic and dynamic modeling for the dual-stage GSPs; Section 3 describes the controller design; Section 4 presents the robot system's parameters for simulation; Section 5 discusses results on oscillation regeneration and balance control, followed by conclusions.

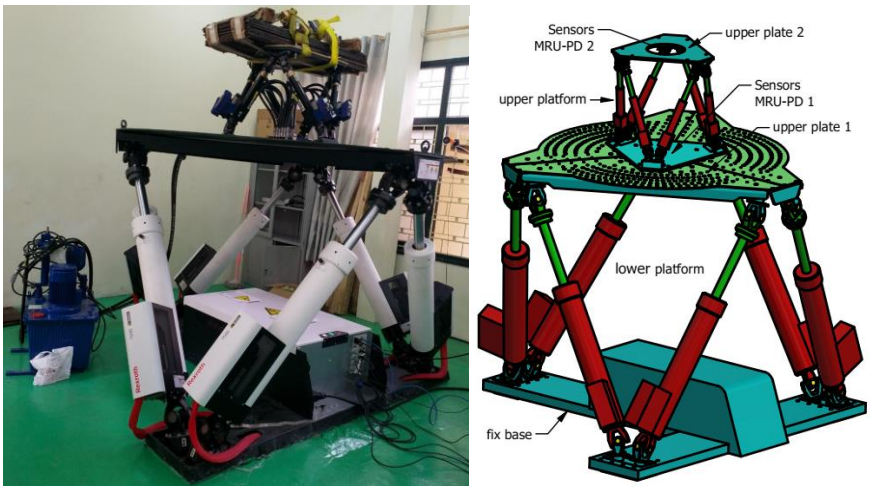

Fig. 1. The dual-stage Gough-Stewart platforms

2. KINEMATIC AND DYNAMIC MODELING

2.1. KINEMATIC MODELING OF THE DUAL-STAGE GSP

To derive the kinematic equations for the dual-stage GSP, coordinate frames must be attached to the robot's links (Fig. 2a shows the kinematic diagram of the two-stage GSPs, and Fig. 2b shows the kinematic diagram of a single GSP at the *k-th* stage, with *k=1,2*).

The base plate of the k-th robot is denoted as B_k, the work plate (upper plate) of the *k-th* robot is denoted as P_k. The center of the joints on the base plate B_k is labeled as B_{ki} ($i=1..6$), and the center of the joints on the upper plate Pk is labeled as P_{ki} ($i=1..6$).

The base frame $O_0x_0y_0z_0$ is attached at the center of the base plate of the lower platform, with the z_0 axis perpendicular to the plate B_k and pointing upwards, and the x_0 axis passing through the midpoint of the line connecting joints B_{k1} and B_{k6}. The frames $O_kx_ky_kz_k$ ($k=1,2$) are attached to the work plates of the corresponding platform at stage 1 and stage 2, where the z_k axis is perpendicular to the plate P_k and points upwards, and the x_k passes through the midpoint of the line connecting joints P_{k1} and P_{k6}. The distance from the center of the plates to the joint centers on the corresponding plates are a_{1i}, b_{1i}, a_{2i}, b_{2j}, respectively. The leg lengths of the robots at levels 1 and 2 are denoted as d_{1i}, d_{2j}, where $i, j = 1,..,6$.

The frame $B_{ki}x_{k-1,i}y_{k-1,i}z_{k-1,i}$ is attached to the base plate (lower plate), with the origin at the center of the *i-th* joint; the axis $B_{ki}x_{k-1,i}$ coincides with $O_{k-1}B_{ki}$; the axis $B_{ki}z_{k-1,i}$ is perpendicular to the plane of the base plate and points upwards. The frame $P_{ki}x_{pi}y_{pi}z_{pi}$ is attached to the plate P_k, with the origin at the center of the *i-th* joint; the axis $P_{ki}x_{pi}$ coincides with O_kP_{ki}; the axis $P_{ki}z_{pi}$ is perpendicular to the plate P_k, see Fig. 2b.

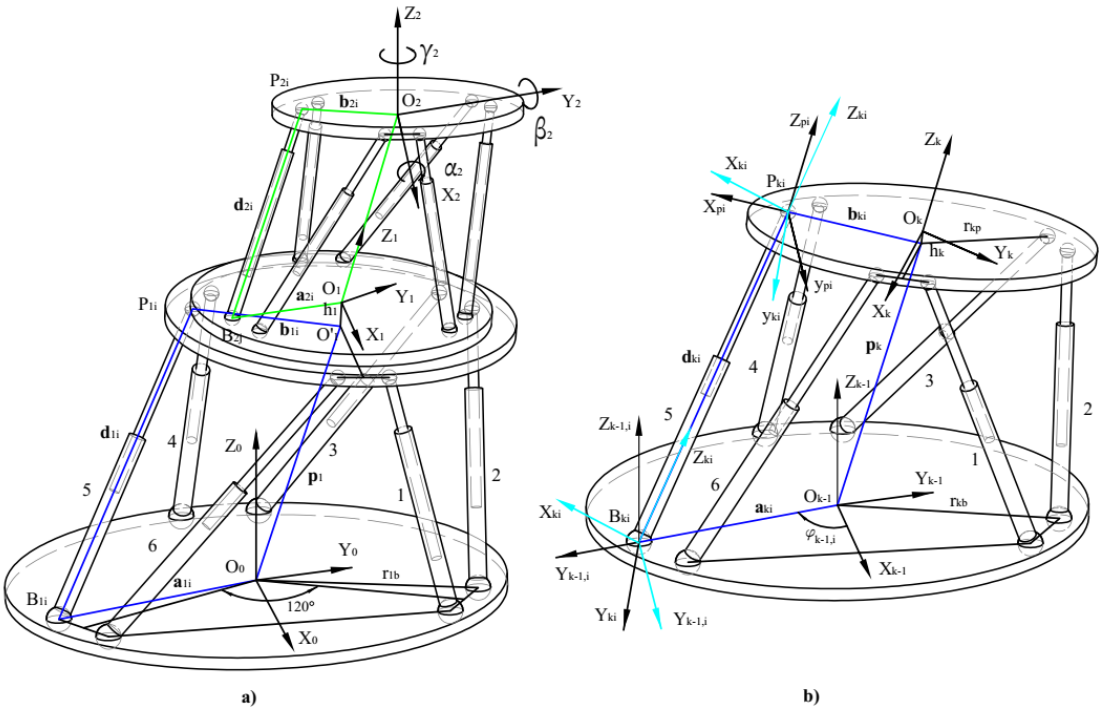

Fig. 2. The dual-stage Gough-Stewart platforms

The generalized coordinate vectors, which define the orientation and position in the workspace of the work plates of robots 1 and 2, are denoted as $\mathbf{p}_1$, $\mathbf{p}_2$, respectively:

$$\mathbf{p}_k = \begin{bmatrix} x_k & y_k & z_k & \alpha_k & \beta_k & \gamma_k \end{bmatrix}^T, \; k = 1,2 \tag{1}$$

The generalized coordinate vectors in the joint space of the robots 1 and 2 is:

$$\mathbf{q}_k = \begin{bmatrix} \mathbf{d}_k & \boldsymbol{\theta}_k & \boldsymbol{\psi}_k \end{bmatrix}^T, \; k = 1,2 \tag{2}$$

Where $\mathbf{d}_k, \boldsymbol{\theta}_k, \boldsymbol{\psi}_k$ is the generalized coordinate vectors with components being the lengths and angles of the legs of the lower and upper platform, respectively.

$$\begin{aligned}
\mathbf{d}_k &= \begin{bmatrix} d_{k1} & d_{k2} & d_{k3} & d_{k4} & d_{k5} & d_{k6} \end{bmatrix}^T \\
\boldsymbol{\theta}_k &= \begin{bmatrix} \theta_{k1} & \theta_{k2} & \theta_{k3} & \theta_{k4} & \theta_{k5} & \theta_{k6} \end{bmatrix}^T, \; k = 1,2 \\
\boldsymbol{\psi}_k &= \begin{bmatrix} \psi_{k1} & \psi_{k2} & \psi_{k3} & \psi_{k4} & \psi_{k5} & \psi_{k6} \end{bmatrix}^T
\end{aligned} \tag{3}$$

Consider the kinematic loop of the i-th leg at stage k of the robot, as shown in Fig. 3. The coordinates of point P in the O_{k-1} frame is determined in two ways, corresponding to two paths. The transformation from the frame $O_{k-1}x_{k-1}y_{k-1}z_{k-1}$ to the frame $P_{ki}x_{ki}y_{ki}z_{ki}$ through the two paths is as follows:

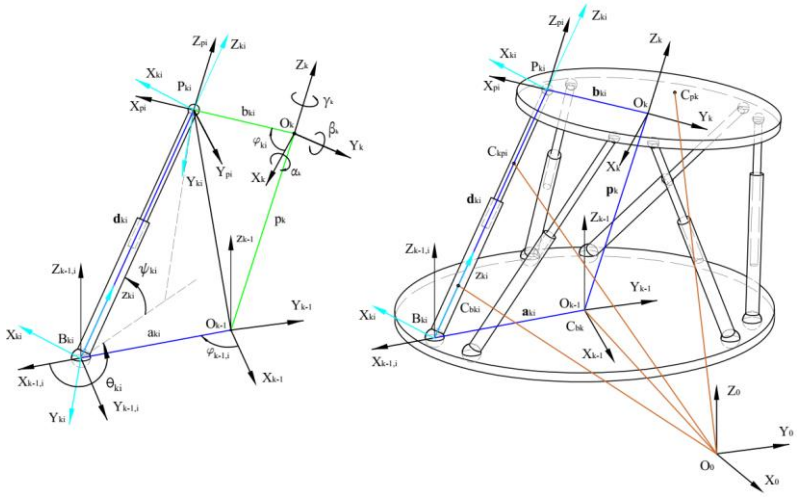

Fig. 3. The dual-stage Gough-Stewart platforms

Path 1: Rotate the frame $O_{k-1}x_{k-1}y_{k-1}z_{k-1}$ around the z_{k-1} axis by an angle φ_{ki}, then translate along the $x_{k-1,i}$ axis by a distance r_{kb}. Rotate the frame $B_{ki}x_{k-1,i}y_{k-1,i}z_{k-1,i}$ around the $B_{ki}x_{k-1,i}$, $B_{ki}y_{k-1,i}$, axes by the angles θ_{ki}, ψ_{ki}. Translate $B_{ki}x_{ki}y_{ki}z_{ki}$ along the z_{ki} axis by a distance d_{ki}.

Path 2: Perform three basic rotations by angles α_k, β_k, γ_k and three basic translations along the x_{k-1}, y_{k-1}, z_{k-1} axes to take the frame $O_{k-1}x_{k-1}y_{k-1}z_{k-1}$ into alignment with the frame $O_kx_ky_kz_k$. Rotate the frame $O_kx_ky_kz_k$ around the z_k axis by an angle φ_{ki}, then translate along the x_k axis by a distance r_{kb}.

Following the two kinematic paths at the *i-th* leg, by determining the homogeneous transformation matrices at each step and multiplying the transformation matrices together, we obtain the homogeneous matrices that determine the position and orientation of the frame $P_{ki}x_{ki}y_{ki}z_{ki}$ relative to the frame $O_{k-1}x_{k-1}y_{k-1}z_{k-1}$ as follows:

$$\begin{aligned}
{}^{k-1}\mathbf{A}_{1,ki} &= {}^{k-1}\mathbf{A}_{k-1,i}\left(r_{kb}, \varphi_{k-1,i}\right) {}^{k-1,i}\mathbf{A}_{ki}\left(\psi_{ki}, \theta_{ki}, d_{ki}\right) \\
{}^{k-1}\mathbf{A}_{2,ki} &= {}^{k-1}\mathbf{A}_{k}\left(x_k, y_k, z_k, \alpha_k, \beta_k, \gamma\right) {}^{k}\mathbf{A}_{ki}\left(r_{kp}, \varphi_{ki}\right); \; k = 1,2; \; i = \overline{1,6}
\end{aligned} \tag{4}$$

From (4), since the position of point P_{ki} calculated from both paths is the same, we obtain three equations based on the position of point P_{ki} as follows:

$$\begin{cases} f_{i1} = {}^{k-1}\mathbf{A}_{1,ki}[1,4] - {}^{k-1}\mathbf{A}_{2,ki}[1,4] \\ f_{i3} = {}^{k-1}\mathbf{A}_{1,ki}[2,4] - {}^{k-1}\mathbf{A}_{2,ki}[2,4] \;; i = 1,..,6 \\ f_{i3} = {}^{k-1}\mathbf{A}_{1,ki}[3,4] - {}^{k-1}\mathbf{A}_{2,ki}[3,4] \end{cases} \tag{5}$$

Thus, for each kinematic loop of the *i-th* leg, we have 3 equations. Since a single platform of the robot has 6 legs, there are a total of 18 equations:

$$\mathbf{f}_k(\mathbf{q}_k) = \mathbf{f}_k(\mathbf{p}_k);\ \mathbf{q}_k = \left[\psi_{ki}, \theta_{ki}, d_{ki}\right]^T;\ i = 1,..,6;\ k = 1,2; \mathbf{p}_k = \left[x_k, y_k, z_k, \alpha_k, \beta_k, \gamma_k\right]^T \tag{6}$$

Equation (6) can be simplified to the following form:

$$\begin{aligned} &\mathbf{f}_k(\mathbf{q}_k, \mathbf{p}_k) = \mathbf{f}_{18x1}(\mathbf{q}_k, \mathbf{p}_k) = \mathbf{f}_k(\mathbf{X}_k) = 0 \\ &\mathbf{X}_k = (\mathbf{q}_k, \mathbf{p}_k);\quad k = 1,2 \end{aligned} \tag{7}$$

Considering both levels of the robot, *k=1, 2*, we obtain the generalized kinematic equations of the two-stage robot system, consisting of 36 equations.

Kinematic problems: The kinematic problems of a multi-stage platform include the forward kinematics problem, the inverse kinematics problem. The forward kinematics problem is to determine the position and orientation of the work plate (workspace variables $\boldsymbol{p}_k$) from the known joint variables (joint space variables $\boldsymbol{q}_k$ or $\boldsymbol{d}_k$), at a specific stage of the robot system. The inverse kinematics problem is to compute the variables in the joint space (find $\boldsymbol{d}_k$, $\boldsymbol{q}_k$), given the desired motion of the work plate (given $\boldsymbol{p}_k$).

Velocities computation: The velocities of the rigid bodies (links) in the robot system are generally calculated for the *k-th* stage of the robot. By differentiating the first equation of equation (6), we obtain:

$$\sum_{i=1}^{18} \frac{\partial \mathbf{f}_{k\xi}}{\partial \mathbf{p}_{ki}} \dot{\mathbf{p}}_{ki} = -\sum_{j=1}^{6} \frac{\partial \mathbf{f}_{k\xi}}{\partial \mathbf{q}_{kj}} \dot{\mathbf{q}}_{kj}\ ;\ \xi = 1,...,18 \Leftrightarrow \mathbf{J}_{Pk} \dot{\mathbf{p}}_k = \mathbf{J}_{qk} \dot{\mathbf{q}}_k \tag{8}$$

From (8), the velocities of the generalized coordinates in the joint space can be calculated:

$$\dot{\mathbf{q}}_k = \mathbf{J}_{qk}^{-1} \mathbf{J}_{pk} \dot{\mathbf{p}}_k \tag{9}$$

Accelerations computation:

Differentiate equations (8) with respect to time:

$$\sum_{j=1}^{18} \sum_{i=1}^{18} \frac{\partial^2 \mathbf{f}_{k\xi}}{\partial \mathbf{p}_{ki} \partial \mathbf{p}_{kj}} \dot{\mathbf{p}}_{ki} \dot{\mathbf{p}}_{kj} + \sum_{i=1}^{18} \frac{\partial \mathbf{f}_{k\xi}}{\partial \mathbf{p}_{ki}} \ddot{\mathbf{p}}_{ki} = -\sum_{s=1}^{6} \sum_{l=1}^{6} \frac{\partial^2 \mathbf{f}_{k\xi}}{\partial \mathbf{q}_{ks} \partial \mathbf{q}_{sl}} \dot{\mathbf{q}}_{ks} \dot{\mathbf{q}}_{kl} + \sum_{s=1}^{6} \frac{\partial \mathbf{f}_{k\xi}}{\partial \mathbf{q}_{ks}} \ddot{\mathbf{q}}_{ks},\ \xi = 1,..,18 \tag{10}$$

Equation (10) is rewritten in the following form:

$$\begin{aligned} &\mathbf{J}_{pk} \ddot{\mathbf{p}}_k = \mathbf{g}_k;\ \mathbf{g}_k = \left[\mathbf{g}_{k1},\ \mathbf{g}_{k2},\ .\ .\ .\ \mathbf{g}_{k18}\right] \\ &\mathbf{g}_{k\xi} = -\sum_{j=1}^{18} \sum_{i=1}^{18} \frac{\partial^2 \mathbf{f}_{k\xi}}{\partial \mathbf{p}_{ki} \partial \mathbf{p}_{kj}} \dot{\mathbf{p}}_{ki} \dot{\mathbf{p}}_{kj} - \sum_{s=1}^{6} \sum_{l=1}^{6} \frac{\partial^2 \mathbf{f}_{k\xi}}{\partial \mathbf{q}_{ks} \partial \mathbf{q}_{sl}} \dot{\mathbf{q}}_{ks} \dot{\mathbf{q}}_{kl} + \sum_{s=1}^{6} \frac{\partial \mathbf{f}_{k\xi}}{\partial \mathbf{q}_{ks}} \ddot{\mathbf{q}}_{ks},\ \xi = 1,..,18 \end{aligned} \tag{11}$$

Differentiate equation (9) to obtain the acceleration of the generalized coordinates in joint space:

$$\ddot{\mathbf{q}}_k = \mathbf{J}_{qk}^{-1} \mathbf{J}_{pk} \ddot{\mathbf{p}}_k + \mathbf{J}_{qk}^{-1} \dot{\mathbf{J}}_{pk} \dot{\mathbf{p}}_k - \mathbf{J}_{qk}^{-1} \dot{\mathbf{J}}_{qk} \dot{\mathbf{q}}_k \tag{12}$$

2.2. DYNAMIC MODELING OF THE K-TH-STAGE GSP

For convenience in presenting dynamic modeling method of the two-stage GSPs, the dynamic model of the *k-th* stage GSP is derived first; then, the dynamic model of the two-stage GSPs is combined and solved simultaneously.

This section presents the dynamic modeling for the k-th stage of the robot as shown in Fig.1b. The generalized coordinates and the first and second derivatives of the generalized coordinates for the k-th stage of the robot in the dynamic problem include 18 joint variables, represented in the algebraic vector $\boldsymbol{q}_k$, and 6 generalized coordinate variables of the work plate P_k, represented in the algebraic vector $\boldsymbol{p}_k$.

Applying the Lagrange equations of motion with Lagrange multipliers, the dynamic state of the *k-th* stage robot system is described by the constraint equations (6) and the differential equations of motion:

$$\begin{cases} \mathbf{M}_k\left(\mathbf{X}_k\right)\ddot{\mathbf{X}}_k + \mathbf{C}_k\left(\mathbf{X}_k, \dot{\mathbf{X}}_k\right)\dot{\mathbf{X}} + \mathbf{P}_k\left(\mathbf{X}_k\right) + \mathbf{Q}_k\left(\mathbf{X}_k\right) + \mathbf{U}^*_k = \mathbf{U}_k \\ \mathbf{f}_k\left(\mathbf{X}_k\right) = 0, \ k = 1,2 \end{cases} \tag{13}$$

Where: $\mathbf{X}_k, \dot{\mathbf{X}}_k, \ddot{\mathbf{X}}_k$ are the generalized coordinate vector, its first and second time derivatives, respectively:

$$\mathbf{X}_k = (\mathbf{q}_k, \mathbf{p}_k); \ \dot{\mathbf{X}}_k = (\dot{\mathbf{q}}_k, \dot{\mathbf{p}}_k); \ \ddot{\mathbf{X}}_k = (\ddot{\mathbf{q}}_k, \ddot{\mathbf{p}}_k) \tag{14}$$

$\boldsymbol{M_k(X_k)}$ is the generalized mass matrix:

$$\mathbf{M}_k\left(\mathbf{X}_k\right) = \begin{bmatrix} m_{k1,1} & m_{k1,2} & \ldots & m_{k1,24} \\ \ldots & \ldots & \ldots & \ldots \\ m_{k24,1} & m_{k24,2} & \ldots & m_{k24,24} \end{bmatrix} \tag{15}$$

The matrix $\boldsymbol{M_k(X_k)}$ is calculated as follows:

$$\mathbf{M}_k(\mathbf{X}_k) = \sum_{i=1}^{n}\left(m_{ki}\mathbf{J}_{Ti}^T\mathbf{J}_{Ti} + \mathbf{J}_{Ri}^T\mathbf{I}_i\mathbf{J}_{Ri}\right); \ \mathbf{J}_{Ti} = \frac{\partial \mathbf{r}_{Ci}}{\partial \mathbf{X}_k}; \ \mathbf{J}_{Ti} = \frac{\partial \boldsymbol{\omega}_i}{\partial \mathbf{X}_k} \tag{16}$$

With n being the number of moving links at stage k, m_i is the mass of the i-th moving link. $\boldsymbol{J_{Ti}}$, $\boldsymbol{J_{Ri}}$ are the translational Jacobian matrix and the rotational Jacobian matrix of the *i-th* moving link. These matrices are calculated based on the position of the center of mass and the angular velocity of the links. $\boldsymbol{I}_i$ is the inertia tensor of the link with respect to the coordinate system located at the center of mass.

The angular velocity of the i link in the system is calculated using the skew symmetric matrix, through the direction cosine matrix A_i of link i:

$$\tilde{\boldsymbol{\omega}}_i(\mathbf{X}_k, \dot{\mathbf{X}}_k) = \mathbf{A}_i^T\dot{\mathbf{A}}_i = \begin{bmatrix} 0 & -\omega_{iz} & \omega_{iy} \\ \omega_{iz} & 0 & -\omega_{ix} \\ -\omega_{iy} & \omega_{ix} & 0 \end{bmatrix} \tag{17}$$

$\mathbf{C}_k(\mathbf{X}_k, \dot{\mathbf{X}}_k)$ is the centrifugal and Coriolis matrix, is function of the generalized coordinates and velocities $\mathbf{X}_k, \dot{\mathbf{X}}_k$:

$$\mathbf{C}_k(\mathbf{X}_k, \dot{\mathbf{X}}_k) = \frac{\partial \mathbf{M}_k\left(\mathbf{X}_k\right)}{\partial \mathbf{X}_k}\left(\mathbf{E}_n \otimes \dot{\mathbf{X}}_k\right) - \frac{1}{2}\left(\frac{\partial \mathbf{M}_k\left(\mathbf{X}_k\right)}{\partial \mathbf{X}_k}\left(\dot{\mathbf{X}}_k \otimes \mathbf{E}_n\right)\right)^T \tag{18}$$

Where $\boldsymbol{E}_n$ is the unit matrix of size [24x24].

$\boldsymbol{P}_k$ is the [24x1] vector of generalized forces due to potential forces:

$$\mathbf{P}_k(\mathbf{X}_k) = \left(\frac{\partial \mathbf{\Pi}_k}{\partial \mathbf{X}_k}\right)^T \tag{19}$$

Where $\mathbf{\Pi}_k$ is the potential energy of the system.

$\mathbf{Q}_k$ is the [24x1] vector of generalized forces due to non-conservative forces:

$$\mathbf{Q}_k = \left[\mathbf{Q}_{k1}, \mathbf{Q}_{k2}, .., \mathbf{Q}_{k23}, \mathbf{Q}_{k24}\right]^T \tag{20}$$

$\mathbf{U}_k$* is the [1x24] vector whose elements are the generalized forces of the constraint forces at the joints:

$$\mathbf{U}_k = \left[\mathbf{U}^*_{k1}, \mathbf{U}^*_{k2}, ..., \mathbf{U}^*_{k23}, \mathbf{U}^*_{k24}\right]^T \tag{21}$$

$\mathbf{U}_k$ is the [1x24] vector, with elements representing the driving forces at the legs:

$$\mathbf{U}_k = \left[\mathbf{U}_{k1}, \mathbf{U}_{k2}, ...\mathbf{U}_{k6}, 0, 0, 0, ..., 0, 0, 0\right]^T \tag{22}$$

The solution of the dynamic equations (13) are performed when the dynamic components in the system are computed.

The forward dynamics problem of the robot: Given the driving forces at the legs and external forces acting on the robot, determine the motion of the work plate.

By differentiating the constraint equations twice with respect to time, from (13) we have:

$$\begin{cases} \mathbf{M}_k(\mathbf{X}_k)\ddot{\mathbf{X}}_k + \mathbf{C}_k(\mathbf{X}_k, \dot{\mathbf{X}}_k)\dot{\mathbf{X}}_k + \mathbf{P}_k(\mathbf{X}_k) + \mathbf{Q}_k + \mathbf{U}^*_k = \mathbf{U}_k \\ \mathbf{G}_k(\mathbf{X}_k)\ddot{\mathbf{X}}_k = \mathbf{g}_k(\mathbf{X}_k, \dot{\mathbf{X}}_k) \end{cases} \tag{23}$$

The constraint forces can be expressed in the form of Lagrange multipliers as follows:

$$\mathbf{U}^*_k = \mathbf{G}^T_k \boldsymbol{\lambda}_k \tag{24}$$

$$\text{Where } \mathbf{G}_k = \begin{bmatrix} \frac{\partial f_{k1}}{\partial X_{k1}} & \cdots & \frac{\partial f_{k1}}{\partial X_{k24}} \\ \cdots & \cdots & \cdots \\ \frac{\partial f_{k18}}{\partial X_{k1}} & \cdots & \frac{\partial f_{k18}}{\partial X_{k24}} \end{bmatrix} \tag{25}$$

Substituting into equation (22) and writing in matrix form, we have:

$$\begin{bmatrix} \mathbf{M}_k(\mathbf{X}_k) & \mathbf{G}^T_k(\mathbf{X}_k) \\ \mathbf{G}_k(\mathbf{X}_k) & 0 \end{bmatrix} \begin{bmatrix} \ddot{\mathbf{X}}_k \\ \boldsymbol{\lambda}_k \end{bmatrix} = \begin{bmatrix} -\mathbf{C}_k(\mathbf{X}_k, \dot{\mathbf{X}}_k)\dot{\mathbf{X}}_k - \mathbf{P}_k(\mathbf{X}_k) - \mathbf{Q}_k + \mathbf{U}_k \\ \mathbf{g}_k(\mathbf{X}_k, \dot{\mathbf{X}}_k) \end{bmatrix} \tag{26}$$

The equations (26) have 42 equations, with 42 unknowns consisting of 24 unknowns for the generalized coordinates, their first and second derivatives, and 18 Lagrange multipliers λ_k.

The inverse dynamics problem: Calculating the inverse dynamics is an important task in controlling the parallel robot system to meet the specified requirements. Given the motion of the work plate $\mathbf{p}_k, \dot{\mathbf{p}}_k, \ddot{\mathbf{p}}_k$ and the external forces $\mathbf{P}_k$, $\mathbf{Q}_k$ find the motion $\mathbf{q}_k, \dot{\mathbf{q}}_k, \ddot{\mathbf{q}}_k$ and driving forces $\mathbf{U}_k$ at the legs. The motions of the robot legs are solved using the inverse kinematics, where the unknowns in the inverse dynamics include the 6 driving forces variables in $\mathbf{U}_k$ and 18 Lagrange multipliers in $\boldsymbol{\lambda}_k$.

Rewriting the expression $\mathbf{U}_k^* = -\mathbf{G}_k^{*T}\boldsymbol{\lambda}_k$ and substituting it into the first equation of (13), we have:

$$\mathbf{M}_k\left(\mathbf{X}_k\right)\ddot{\mathbf{X}}_k + \mathbf{C}_k\left(\mathbf{X}_k,\dot{\mathbf{X}}_k\right)\dot{\mathbf{X}}_k + \mathbf{P}_k\left(\mathbf{X}_k\right) + \mathbf{Q}_k\left(\mathbf{X}_k\right) = \mathbf{G}_k^{*T}\left(\mathbf{X}_k\right)\boldsymbol{\lambda}_k + \mathbf{U}_k \tag{27}$$

The equations (13) become:

$$\begin{cases} \mathbf{M}_k\left(\mathbf{X}_k\right)\ddot{\mathbf{X}}_k + \mathbf{C}_k\left(\mathbf{X}_k,\dot{\mathbf{X}}_k\right)\dot{\mathbf{X}}_k + \mathbf{P}_k\left(\mathbf{X}_k\right) + \mathbf{Q}_k\left(\mathbf{X}_k\right) = \mathbf{K}_k\mathbf{y}_k \\ \mathbf{f}_k\left(\mathbf{X}_k\right) = \mathbf{0} \end{cases} \tag{28}$$

$$\text{Where: } \mathbf{K}_k = \begin{bmatrix} \mathbf{E}_{6c6} & \mathbf{G}_{k\,[24x18]}^{*T} \\ \mathbf{0}_{18x6} & \end{bmatrix}_{24x24}; \mathbf{y}_k = \left[U_{k1}, U_{k2}, .., U_{k6}, \lambda_{k1}, \lambda_{k2}, .., \lambda_{k18}\right]^T \tag{29}$$

To compute the inverse dynamic equations (28), the inverse kinematics problem in the second equation is computed first, and then substituted into the first equation to determine the driving forces and Lagrange multipliers, as well as the constraint forces.

Dynamic modeling of the dual-stage GSPs

The dynamic equation (13) combined for the two-stage GSPs is written as follows:

$$\begin{cases} \mathbf{M}(\mathbf{X})\ddot{\mathbf{X}} + \mathbf{C}(\mathbf{X},\dot{\mathbf{X}})\dot{\mathbf{X}} + \mathbf{P}(\mathbf{X}) + \mathbf{Q}(\mathbf{X}) + \mathbf{U}^* = \mathbf{U} \\ \mathbf{f}(\mathbf{X}) = \mathbf{0} \end{cases} \tag{30}$$

Where:

$$\mathbf{X}_{48x1} = \begin{bmatrix} \mathbf{X}_1 \\ \mathbf{X}_2 \end{bmatrix};\ \dot{\mathbf{X}} = \begin{bmatrix} \dot{\mathbf{X}}_1 \\ \dot{\mathbf{X}}_2 \end{bmatrix};\ \ddot{\mathbf{X}} = \begin{bmatrix} \ddot{\mathbf{X}}_1 \\ \ddot{\mathbf{X}}_2 \end{bmatrix} \mathbf{M}_{48x48} = \begin{bmatrix} \mathbf{M}_1 \\ \mathbf{M}_2 \end{bmatrix}; \mathbf{C}_{48x48} = \begin{bmatrix} \mathbf{C}_1 \\ \mathbf{C}_2 \end{bmatrix}; \mathbf{P}_{48x1} = \begin{bmatrix} \mathbf{P}_1 \\ \mathbf{P}_2 \end{bmatrix};$$
$$\mathbf{Q}_{48x1} = \begin{bmatrix} \mathbf{Q}_1 \\ \mathbf{Q}_2 \end{bmatrix};\ \mathbf{U}_{48x1}^* = \begin{bmatrix} \mathbf{U}_1^* \\ \mathbf{U}_2^* \end{bmatrix}; \mathbf{U}_{48x1} = \begin{bmatrix} \mathbf{U}_1 \\ \mathbf{U}_2 \end{bmatrix}; \mathbf{f}_{36x1}\left(\mathbf{X}\right) = \begin{bmatrix} \mathbf{f}_1\left(\mathbf{X}_1\right) \\ \mathbf{f}_2\left(\mathbf{X}_2\right) \end{bmatrix} \tag{31}$$

The equations of motion (30) have 84 equations, with 84 unknowns consisting of 48 unknowns for the generalized coordinates, their first and second derivatives, and 36 Lagrange multipliers $\boldsymbol{\lambda}$.

3. PD CONTROL WITH FORCES COMPENSATION IN TASK SPACE

To design the PD controller with forces compensation in the task space, the dynamic equations should be simplified into a compact form that represents the relationship between the driving force at the legs and the variables in the task space. This requires eliminating the Lagrange multipliers, following the method presented in [15]. As previously, the equations are first simplified for a single platform, then extended to the entire system for clarity in the derivation.

From (9), we deduce:

$$\dot{\mathbf{X}}_k = \begin{bmatrix} \dot{\mathbf{q}}_k \\ \dot{\mathbf{p}}_k \end{bmatrix} = \begin{bmatrix} \mathbf{J}_{qk}^{-1}\mathbf{J}_{pk} \\ \mathbf{E} \end{bmatrix} \dot{\mathbf{p}}_k = \mathbf{H}_k\dot{\mathbf{p}}_k \tag{32}$$

Where $\mathbf{E}_{6x6}$ is the unit matrix.

From equations (12) and (32), we obtain:

$$\ddot{\mathbf{q}}_k = \mathbf{J}_{qk}^{-1}\mathbf{J}_{pk}\ddot{\mathbf{p}}_k + \mathbf{J}_{qk}^{-1}\dot{\mathbf{J}}_{pk}\dot{\mathbf{p}}_k - \mathbf{J}_{qk}^{-1}\dot{\mathbf{J}}_{qk}\mathbf{J}_{qk}^{-1}\mathbf{J}_{pk}\dot{\mathbf{p}}_k \tag{33}$$

Equation (33) can be rewritten in the form:

$$\ddot{\mathbf{X}}_k = \begin{bmatrix}\ddot{\mathbf{q}}_k \\ \ddot{\mathbf{p}}_k\end{bmatrix} = \begin{bmatrix}\mathbf{J}_{qk}^{-1}\mathbf{J}_{pk} \\ \mathbf{E}\end{bmatrix}\ddot{\mathbf{p}}_k + \begin{bmatrix}\mathbf{J}_{qk}^{-1}\dot{\mathbf{J}}_{pk} - \mathbf{J}_{qk}^{-1}\dot{\mathbf{J}}_{qk}\mathbf{J}_{qk}^{-1}\mathbf{J}_{pk} \\ \mathbf{E}\end{bmatrix}\dot{\mathbf{p}}_k = \mathbf{H}_k\ddot{\mathbf{p}}_k + \mathbf{S}_k\dot{\mathbf{p}}_k \tag{34}$$

Multiply both sides of the first equation of (13) by:

$$\mathbf{H}_k^T\mathbf{M}_k\ddot{\mathbf{X}}_k + \mathbf{H}_k^T\mathbf{C}_k\dot{\mathbf{X}}_k + \mathbf{H}_k^T\mathbf{P}_k + \mathbf{H}_k^T\mathbf{Q}_k + \mathbf{H}_k^T\mathbf{G}_k^T\boldsymbol{\lambda}_k = \mathbf{H}_k^T\mathbf{U}_k \tag{35}$$

Since $\mathbf{H}_k\mathbf{G}_k^T\boldsymbol{\lambda}_k = 0$ [15], equation (35) becomes:

$$\mathbf{H}_k^T\mathbf{M}_k\ddot{\mathbf{X}}_k + \mathbf{H}_k^T\mathbf{C}_k\dot{\mathbf{X}}_k + \mathbf{H}_k^T\mathbf{P}_k + \mathbf{H}_k^T\mathbf{Q}_k = \mathbf{H}_k^T\mathbf{U}_k \tag{36}$$

Substitute (9) and (33) into (36):

$$\mathbf{H}_k^T\mathbf{M}_k\mathbf{H}_k\ddot{\mathbf{p}}_k + (\mathbf{H}_k^T\mathbf{M}_k\mathbf{S}_k + \mathbf{H}_k^T\mathbf{C}_k\mathbf{H}_k)\dot{\mathbf{p}}_k + \mathbf{H}_k^T\mathbf{P}_k(\mathbf{X}_k) + \mathbf{H}_k^T\mathbf{Q}_k(\mathbf{X}_k) = \mathbf{H}_k^T\mathbf{U}_k \tag{37}$$

Equation (37) simplifies to:

$$\mathbf{T}_k = \bar{\mathbf{M}}_k\ddot{\mathbf{p}}_k + \bar{\mathbf{C}}_k\dot{\mathbf{p}}_k + \bar{\mathbf{P}}_k + \bar{\mathbf{Q}}_k \tag{38}$$

Where:

$$\bar{\mathbf{M}}_k = \mathbf{H}_k^T\mathbf{M}_k\mathbf{H}_k;\ \bar{\mathbf{C}}_k = (\mathbf{H}_k^T\mathbf{M}_k\mathbf{S}_k + \mathbf{H}_k^T\mathbf{C}_k\mathbf{H}_k);\bar{\mathbf{P}}_k = \mathbf{H}_k^T\mathbf{P}_k;\ \bar{\mathbf{Q}}_k = \mathbf{H}_k^T\mathbf{Q}_k;\ \mathbf{T}_k = \mathbf{H}_k^T\mathbf{U}_k \tag{39}$$

From (38), choose the control law [16, 17]:

$$\mathbf{T}_k = \mathbf{K}_{kP}\mathbf{e}_k + \mathbf{K}_{kD}\dot{\mathbf{e}}_k + \bar{\mathbf{P}}_k + \bar{\mathbf{Q}}_k \tag{40}$$

$\mathbf{e}_k, \dot{\mathbf{e}}_k, \ddot{\mathbf{e}}_k$ are the error vectors for position, orientation, velocity, and acceleration of the work plate of k-th platform, respectively.

$$\mathbf{e}_k = \mathbf{p}_{kd} - \mathbf{p}_k = \left[e_{k1}, e_{k2}, ..., e_{k6}\right]^T;\dot{\mathbf{e}}_k = \dot{\mathbf{p}}_{kd} - \dot{\mathbf{p}}_k = \left[\dot{e}_{k1}, \dot{e}_{k2}, ..., \dot{e}_{k6}\right]^T \tag{41}$$

With the relation as follows:

$$\bar{\mathbf{M}}_k\ddot{\mathbf{p}}_k + \bar{\mathbf{C}}_k\dot{\mathbf{p}}_k = \mathbf{K}_{kP}\mathbf{e}_k + \mathbf{K}_{kD}\dot{\mathbf{e}}_k \tag{42}$$

From (41), with $\left(\ddot{\mathbf{e}}_k = \ddot{\mathbf{p}}_{kd} - \ddot{\mathbf{p}}_k = -\ddot{\mathbf{p}}_k\right)$:

$$-\bar{\mathbf{M}}_k\ddot{\mathbf{e}}_k - \bar{\mathbf{C}}_k\dot{\mathbf{e}}_k = \mathbf{K}_{kP}\mathbf{e}_k + \mathbf{K}_{kD}\dot{\mathbf{e}}_k \Leftrightarrow \ddot{\mathbf{e}}_k + \bar{\mathbf{M}}_k^{-1}(\mathbf{K}_{kD} + \bar{\mathbf{C}}_k)\dot{\mathbf{e}}_k + \bar{\mathbf{M}}_k^{-1}\mathbf{K}_{kP}\mathbf{e}_k \Leftrightarrow \ddot{\mathbf{e}}_k + \bar{\mathbf{K}}_{kD}\dot{\mathbf{e}}_k + \bar{\mathbf{K}}_{kP}\mathbf{e}_k = 0 \tag{43}$$

Where: $\bar{\mathbf{K}}_{kD} = \bar{\mathbf{M}}_k^{-1}(\mathbf{K}_{kD} + \bar{\mathbf{C}}_k);\ \bar{\mathbf{K}}_{kP} = \bar{\mathbf{M}}_k^{-1}\mathbf{K}_{kP}$

The book [17] presents methods for proving system stability based on Lyapunov theory.

$\bar{\mathbf{K}}_{kD}, \bar{\mathbf{K}}_{kP}$ are diagonal and positive definite matrices.

$$\bar{\mathbf{K}}_{kP} = diag(K_{kP1}, K_{kP2}, ..., K_{kPs}), K_{kPs} > 0; \bar{\mathbf{K}}_{kD} = diag(K_{kD1}, K_{kD2}, ..., K_{kDs}),\ K_{kDs} > 0,\ s = 1, 2, ...6 \tag{44}$$

The above expressions for a single platform are combined to expressions for dual-stage GSPs as follows:

$$\mathbf{T} = \bar{\mathbf{M}}\ddot{\mathbf{p}} + \bar{\mathbf{C}}\dot{\mathbf{p}} + \bar{\mathbf{P}} + \bar{\mathbf{Q}} \tag{45}$$

The above expressions for a single platform are combined to expressions for dual-stage GSPs as follows:

$$\mathbf{T}_{12x1} = \begin{bmatrix}\mathbf{T}_1 \\ \mathbf{T}_2\end{bmatrix};\ \dot{\mathbf{X}} = \begin{bmatrix}\dot{\mathbf{X}}_1 \\ \dot{\mathbf{X}}_2\end{bmatrix};\ \ddot{\mathbf{p}} = \begin{bmatrix}\ddot{\mathbf{p}}_1 \\ \ddot{\mathbf{p}}_2\end{bmatrix};\bar{\mathbf{M}}_{12x12} = \begin{bmatrix}\bar{\mathbf{M}}_1 \\ \bar{\mathbf{M}}_2\end{bmatrix};\bar{\mathbf{C}}_{12x12} = \begin{bmatrix}\bar{\mathbf{C}}_1 \\ \bar{\mathbf{C}}_2\end{bmatrix};\bar{\mathbf{P}}_{12x1} = \begin{bmatrix}\bar{\mathbf{P}}_1 \\ \bar{\mathbf{P}}_2\end{bmatrix};\bar{\mathbf{Q}}_{12x1} = \begin{bmatrix}\bar{\mathbf{Q}}_1 \\ \bar{\mathbf{Q}}_2\end{bmatrix}; \tag{46}$$

$$\bar{\mathbf{K}}_{P12x1} = \begin{bmatrix}\bar{\mathbf{K}}_{1P} \\ \bar{\mathbf{K}}_{2P}\end{bmatrix};\bar{\mathbf{K}}_{D12x1} = \begin{bmatrix}\bar{\mathbf{K}}_{1D} \\ \bar{\mathbf{K}}_{2D}\end{bmatrix};\mathbf{e}_{12x1} = \begin{bmatrix}\mathbf{e}_1 \\ \mathbf{e}_2\end{bmatrix};\dot{\mathbf{e}}_{12x1} = \begin{bmatrix}\ddot{\mathbf{e}}_1 \\ \dot{\mathbf{e}}_2\end{bmatrix};\ddot{\mathbf{e}}_{12x1} = \begin{bmatrix}\ddot{\mathbf{e}}_1 \\ \ddot{\mathbf{e}}_2\end{bmatrix} \tag{47}$$

Fig. 4 presents the block scheme of PD control with forces compensation in task space of the dual-stage GSPs. In the control system diagram, the position and velocity of the work plates are measured using MRU-PD Motion Reference Units from Inertial Labs, which are placed on the work plates of the lower and upper platforms. Additionally, the position and orientation of the work plates can be determined from the forward kinematics problem by knowing the values of the joint variables. The external forces acting on the robot can be calculated using the dynamic equations or directly estimated based on the method presented in [18], particularly in cases where the external forces vary and are difficult to calculate.

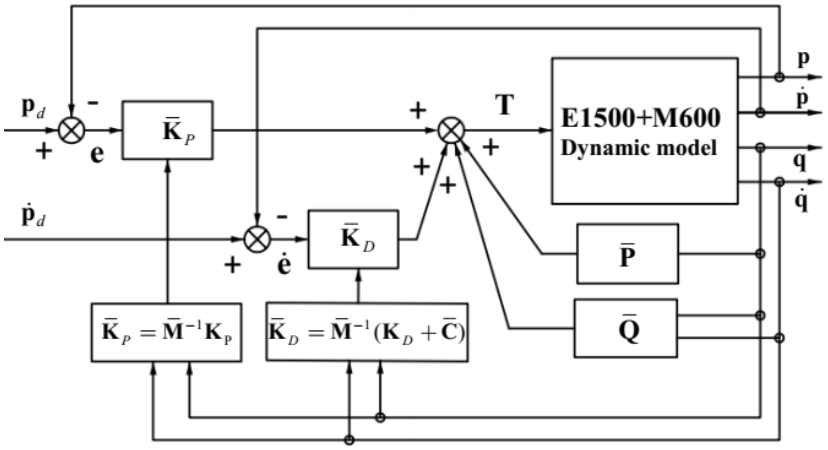

Fig. 4. Block scheme of task space PD control with forces compensation

4. THE KINEMATIC AND DYNAMIC PARAMETERS OF APPLIED ROBOT

The platforms used for computations and simulations include: the GSP at stage 1 is eMotion-1500/2700-6DOF-650-MK1 (referred to as E1500), and the GSP at stage 2 is the MicroMotion 600 (referred to as M600) from Bosch Rexroth, Fig. 1. The kinematic and dynamic parameters of the lower and upper platform are shown in Tab. 1 and Tab. 2.

Table 1. Kinematic parameters of the robot

r_{1b} (m)	r_{1p} (m)	σ_{1b} (deg)	σ_{1p} (deg)	r_{2b} (m)	r_{2p} (m)	σ_{2b} (deg)	σ_{2p} (deg)
1.280	1.101	8.60	20.86	0.354	0.320	14.61	21.56

Table 2. Dynamic parameters of the robot

	m (kg)	x_C (m)	y_C (m)	z_C (m)	Ixx (kgm2)	Iyy (kgm2)	Izz (kgm2)
Cross B_{1i}	2.46	0	0	0	0.0046	0.0035	0.0035
Cyl B_{1i}	150.4	0	0.059	0.544	19.384	18.392	1.539
Pis P_{1i}	31.63	0	0	-0.375	2.632	2.362	0.046
Cross B_{1i}	2.46	0	0	0	0.0046	0.0035	0.0035
Plate P_1	238.2	0	0	0.150	63.384	63.384	135.562
Cross B_{2i}	0.48	0	0	0	3.56e-5	1.18e-5	1.18e-5
Cyl B_{2i}	9.65	0	0	0.168	0.110	0.110	0.006

Pis P_{2i}	3.84	0	0	-0.144	0.020	0.020	0.0008
Cross P_{2i}	0.48	0	0	0	3.56e-5	1.18e-5	1.18e-5
Plate P_2	36.50	0	0	0.120	1.305	1.305	2.566

The moments of inertia in Tab. 2 are calculated with respect to the coordinate frame attached to the center of mass of each corresponding rigid body. The center of mass coordinates are calculated relative to the coordinate frame attached to the local frame, as shown in Figure 2 and Figure 3.

Leg lengths of the E1500 platform: stroke length: 950 mm; minimum leg length: 1306.14 mm; maximum leg length: 2256.14 mm. Leg lengths of the M600 platform: stroke length 350 mm; minimum leg length: 463.6 mm; maximum leg length: 813.6 mm.

Figure 5 shows the diagram created in MATLAB/Simulink in combination with MSCAdams software to compute and simulate the motions of the robot system.

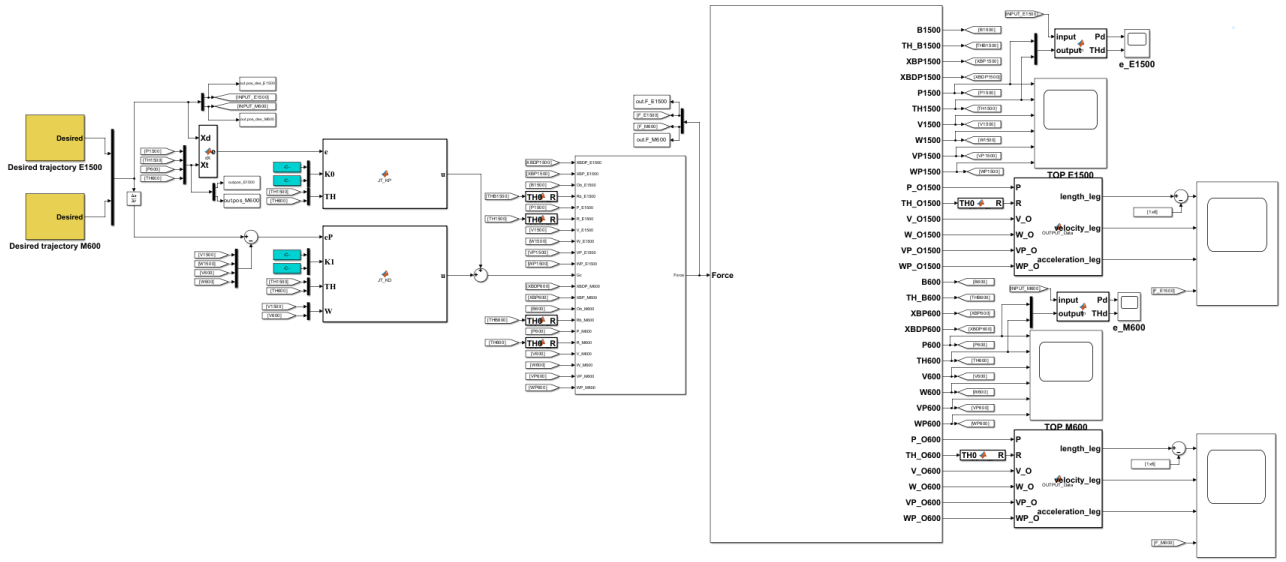

Fig. 5. Robot system diagram in MATLAB/Simulink and MSCAdams

5. COMPUTATION AND SIMULATION RESULT

The PD controller with forces compensation in the task space is applied to the dual-stage platform in the study that the lower platform simulates the oscillations of a ship, while the upper platform maintains stable balance. The controller of E1500 platform is modified with K_{1Pi}=10000, K_{1Di}=1000 (i=*1..6*) and the controller of M600 platform is modified with K_{2Pi}=10000, K_{2Di}=1000 (i=*1..6*).

The inputs of the work plates:

The oscillation generated at the work plate of the E1500 simulates the ship's oscillation on sea waves at sea state 6, presented in [19], Fig. 6. The motion data of the ship is taking from [20], sea state 6, wave type (beta): long-crested (unidirectional), wave coming from bow (front), wave angle: 180 degrees. Ship: HMS Norfolk, dimensions: 137 x15x16m.

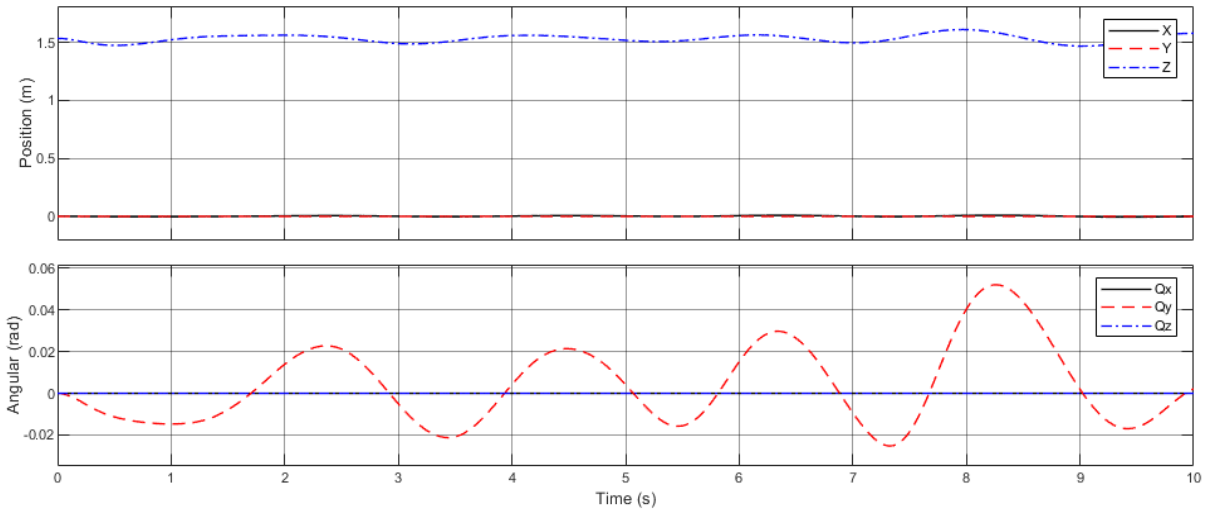

Fig. 6. Oscillations of the ship at sea state 6, wave long-crested [18]

The set balance position and orientation of the work plate of the M600 platform:

$$\mathbf{r}_{P2} = \begin{bmatrix} 0 & 0 & 2.403 & 0 & 0 & 0 \end{bmatrix} \tag{45}$$

In this case, input data of the orientation and position of the lower work plate are in numerical form, velocity is calculated using numerical differentiation.

Computation and simulation results:

With the oscillations of the work plate on the E1500 are regenerated in Fig. 7, the computation program produces results for position, orientation errors, the motion and driving forces of the legs of the E1500 platform, as shown in Fig. 8, 9.

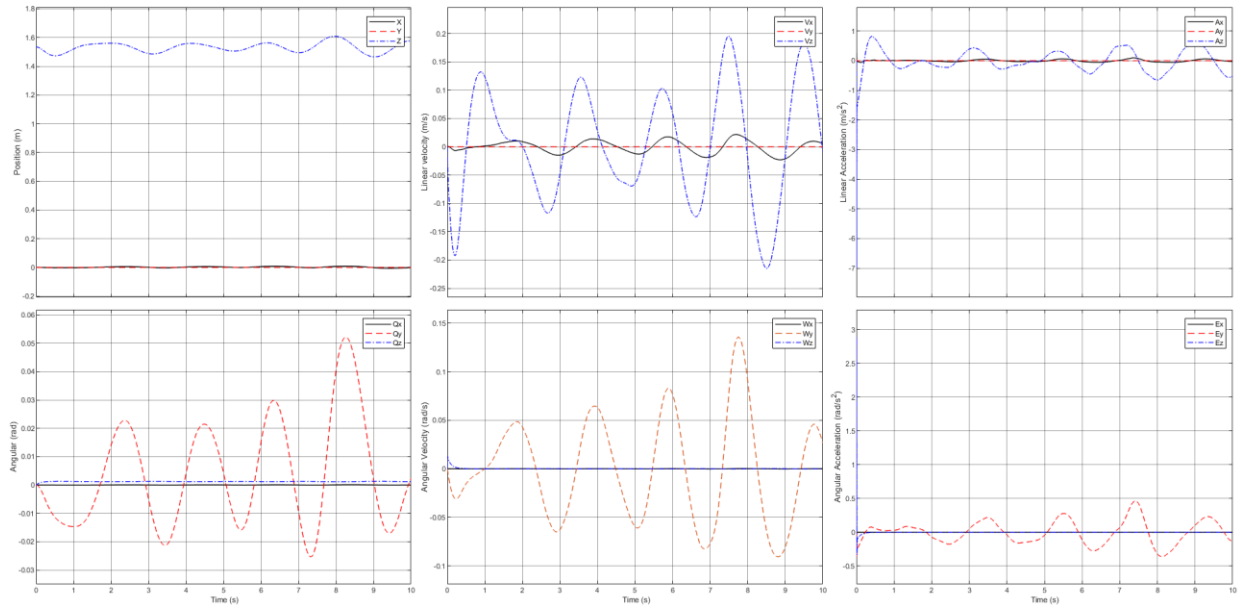

Fig. 7. Oscillations of the work plate of E1500 platform

The set balance position and orientation of the work plate of the M600 (Fig. 10), the errors, motion and driving forces of the legs of the M600 platform, as shown in Fig. 11, 12.

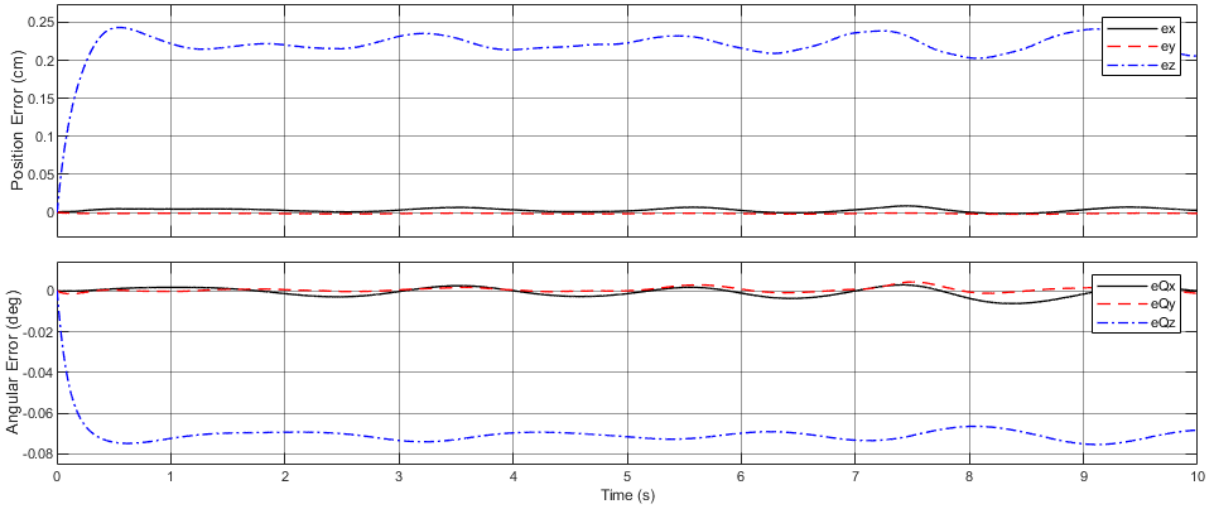

Fig. 8. Position, orientation errors of the work plate of E1500

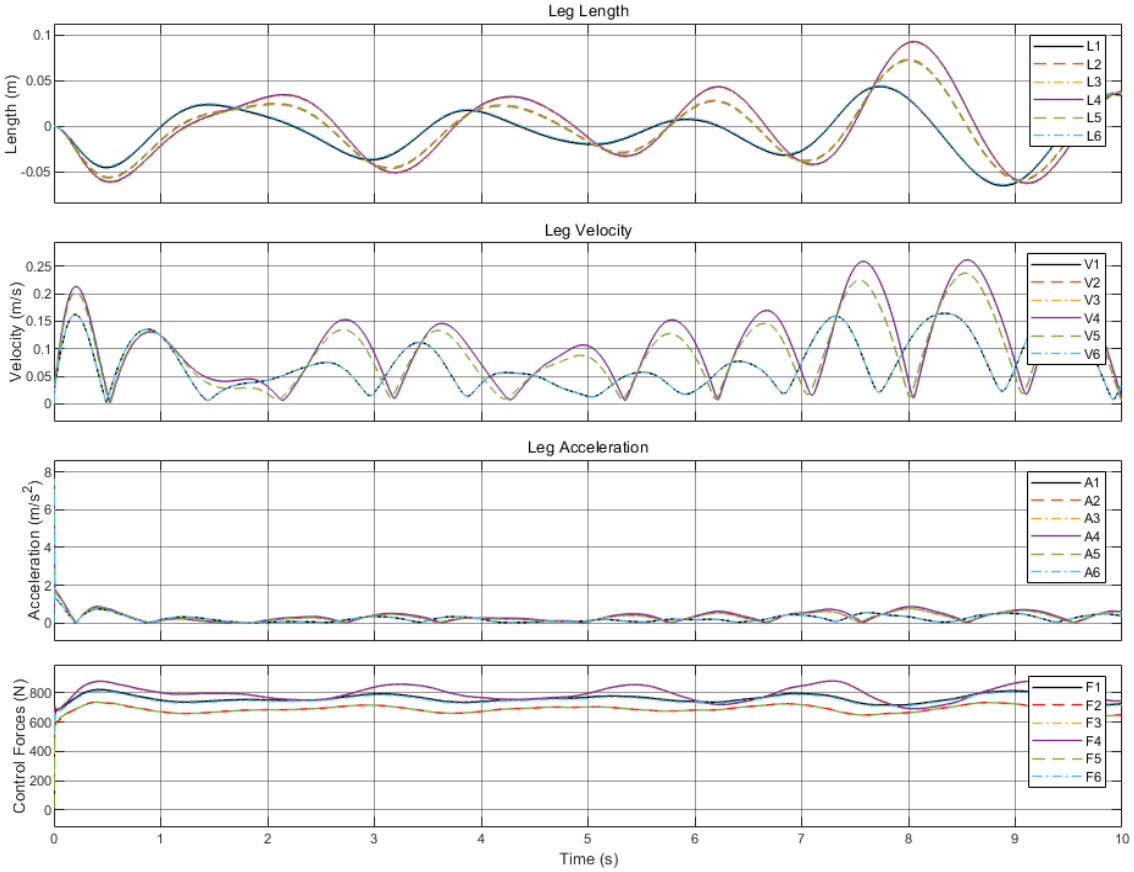

Fig. 9. Position, velocity, acceleration, and forces of the legs of E1500

Simulation results for the E1500 platform: Absolute average position error: 0.2201 cm. Absolute average orientation error: 0.0705 deg. Maximum absolute position error: 0.2432 cm. Maximum absolute orientation error: 0.0754 deg. Maximum control force response: 881.1206 N, Fig.9.

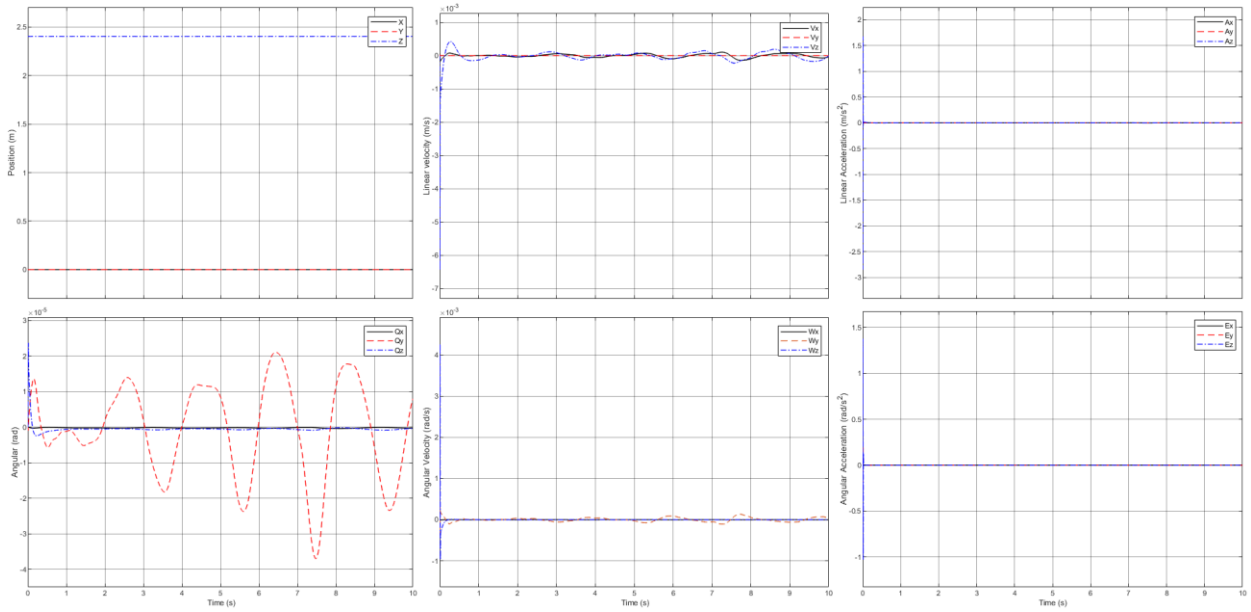

Fig. 10. The work plate of M600 maintains balance

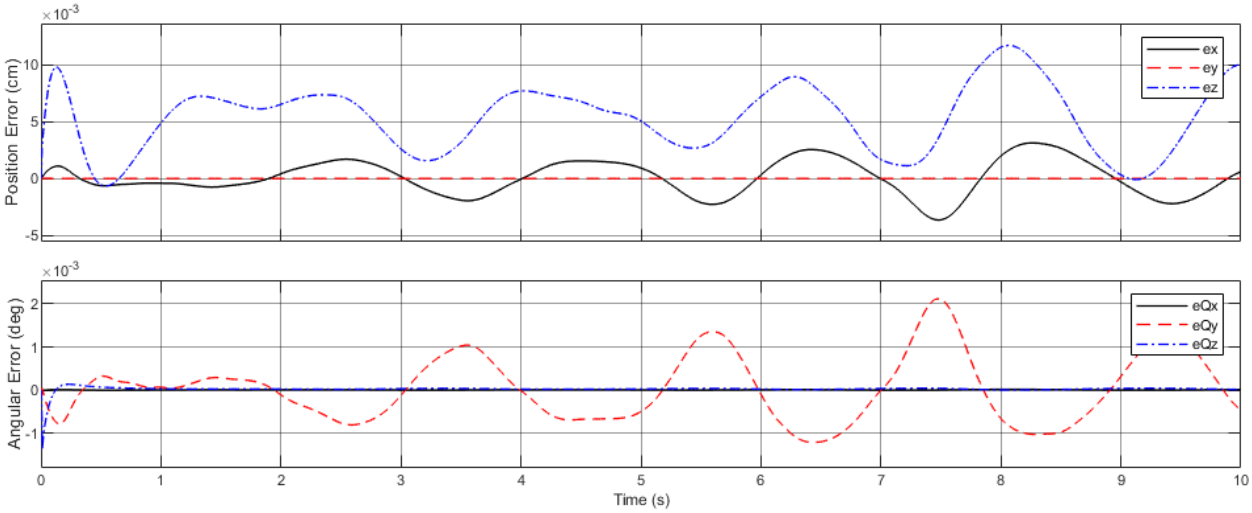

Fig. 11. Balancing errors of the work plate of M600

Simulation results for the M600 platform: Absolute average position error: 0.0056 cm. Absolute average orientation error: 0.0006 deg. Maximum absolute position error: 0.012 cm. Maximum absolute orientation error: 0.0021 deg. Maximum control force response: 103.2423 N, Fig12.

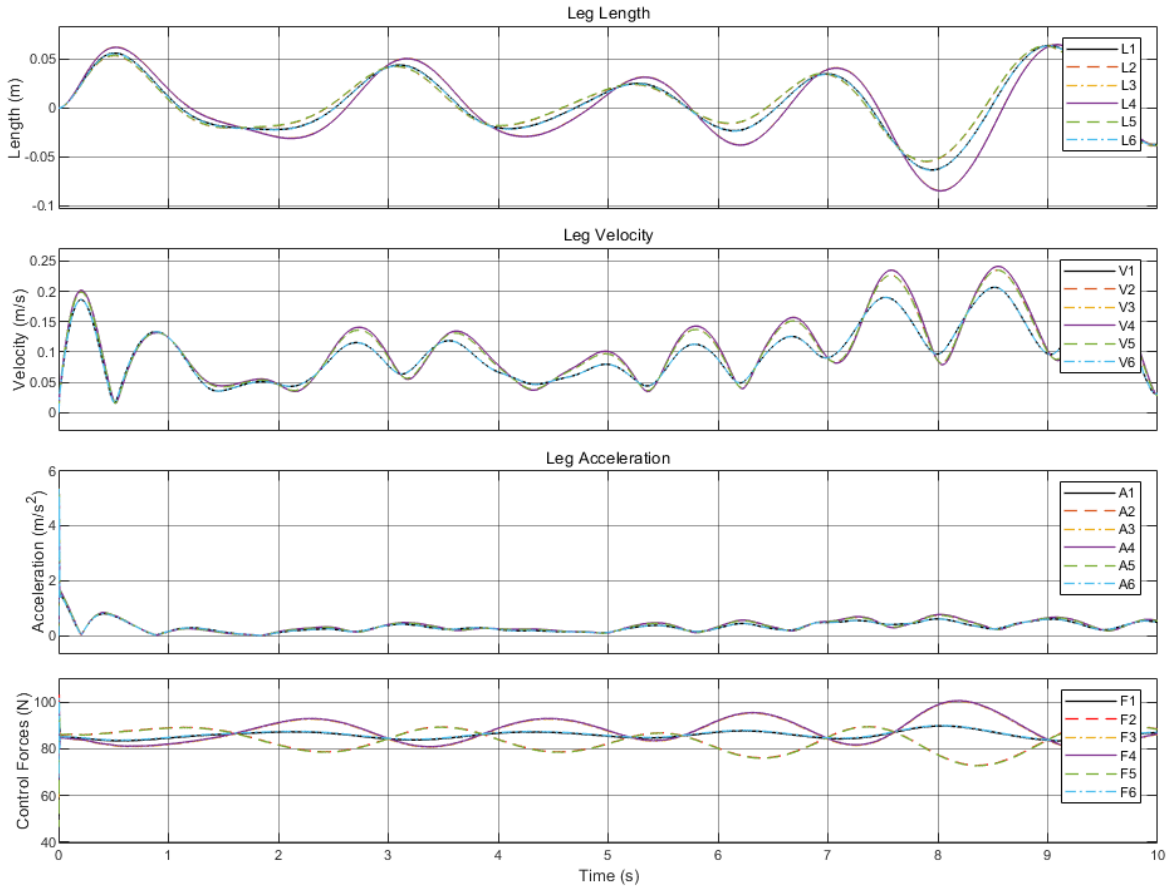

Fig. 12. Position, velocity, acceleration, and forces of the legs of M600

6. CONCLUSIONS

The computation and simulation results indicate that the first platform effectively regenerates the required oscillations, with the motion and driving forces on its legs continuously calculated. The second platform's work plate maintains stable balance around the target position with minimal error, making it suitable for balance stabilization on maritime transportation platforms.

The paper models the kinematics and dynamics of a complex multi-stage parallel robot system with a closed loop structure and a large number degrees of freedom. The kinematic and dynamic equations represent the relationships between driving forces, constraint forces, external forces, and the motions of the legs and work plates across the stages of the robot system, enabling both forward and inverse dynamic analyses.

The PD controller with forces compensation enables oscillation regeneration on the lower platform to simulate vehicle motion, while the upper platform maintains stability.

The results validate the dynamic model's accuracy and the controller's effectiveness, highlighting practical applications for oscillation regeneration and balance stabilization across different vehicles and platforms.

ACKNOWLEDGEMENTS

The authors would like to thank for the use of the eMotion-1500/2700-6DOF-650-MK1 and Micro Motion-600-6DOF-200-MK6 platforms from the Laboratory of the Department of Mechatronics, Faculty of Aerospace Engineering, Le Quy Don Technical University.

REFERENCES

[1] STEWART D., 1965, *A Platform With Six Degrees of Freedom*, Proceedings of the UK Institute of Mechanical Engineering, 180/1, 371–386.
[2] PHAM H.T., NGUYEN V.K., DANG Q.K., DUONG T.V.A., NGUYEN D.T. and PHAN T.V., 2023. *Design Optimization of Compliant Mechanisms for Vibration Assisted Machining Applications Using a Hybrid Six Sigma*, RSM-FEM, and NSGA-II approach, Journal of Machine Engineering, 23/2, 135-138, https://doi.org/10.36897 /jme/166500.
[3] Ampelmann projects, https://www.ampelmann.nl/
[4] SON N.T., CHINH H.Q., NGUYEN D.Q., 2017, *Investigation on Offshore Access Stabilization Systems-Simulation Using the Blockset SimMechanics in Matlab/Simulink*, J. of Science and Technique, Le Quy Don Technical University, 183, 88-100.
[5] MARQUES.F., et al, 2021, *Examination and Comparison of Different Methods to Model Closed Loop Kinematic Chains Using Lagrangian Formulation with Cut Joint, Clearance Joint Constraint and Elastic Joint Approaches*, Mechanism and Machine Theory, 160, 104294.
[6] STAICU S., 2011, *Dynamics of the 6-6 Stewart Parallel Manipulator*, Robotics and Computer Integrated Manufacturing, 27/1, 212-220.
[7] ABDELLATIF H., HEIMANN B., 2009, *Computational Efficient Inverse Dynamics of 6-DOF Fully Parallel Manipulators by Using the Lagrangian Formalism*, Mechanism and Machine Theory, 44, 192-207.
[8] YANG C., HAN J., PETER O. O., HUANG Q., 2011, *PID Control with Gravity Compensation for Hydraulic 6-DOF Parallel Manipulator*, PID Control, Implementation and Tuning, https://doi.org/10.5772/16023.
[9] CAI Y., et al, 2020, *Model Analysis and Modified Control Method of Ship-Mounted Stewart Platforms for Wave Compensation*, IEEE Access, 9, 4505-4517.
[10] TUMELERO V.V., PERONDI E.A., 2017, *Control of an Electrohydraulic Stewart Platform Manipulator for Off-Shore Motion Compensation*, Proceedings of the 3rd International Conference on Mechatronics and Robotics Engineering.
[11] TOURAJIZADEH H., MANTEGHI S., 2016, *Design and Optimal Control of Dual-Stage Stewart Platform Using Feedback-Linearized Quadratic Regulator*, Advanced Robotics, 30/20, 1305-1321.
[12] KHOI P.B., 2010, *Algorithm and Program for Dynamics Calculation of Parallel Robots*, Journal of Science and Technology, 48/1, 33-44.
[13] KHOI P.B., 2005, *Investigation Inverse Kinematics of Parallel Mechanisms in Series Connection*, Proceedings 5th Asian symposium on Applied Electromagnatics and Mechanics, Hanoi, Vietnam, 224-231, (In Vietnamese).
[14] KHOI P.B., HUNG H.H., Hoang Quang Chinh, 2024, *Algorithm and Program for Computing the Kinematics of a Two-Stage Parallel Robot*, Proceedings of the National Mechanics Conference, Vol. 2, pp. 705-714. (In Vietnamese).
[15] VLASE S, 1987, *A Method of Eliminating Lagrangian Multipliers from the Equation of Motion of Interconnected Mechanical Systems*, Journal of Applied Mechanics, March 1987, 235–237, https://doi.org/10.1115/1.3172969.
[16] SCIAVICCO L., BRUNO S., 2012, *Modelling and Control of Robot Manipulators*, Springer Science & Business Media.
[17] KHALIL W., ETIENNE D., 2004, *Modeling, Identification and Control of Robots*, Butterworth-Heinemann.
[18] UHLMANN E., POLTE M., BLUMBERG J., 2023, Estimation of External Force-Torque Vector Based On Double Encoders of Industrial Robots Using a Hybrid Gaussian Process Regression and Joint Stiffness Model, Journal of Machine Engineering, 23/3 36–68, https://doi.org/10.36897/jme/167359.
[19] HUNG H.H., CHINH H.Q., at al, 2022, *Simulation of Vessel Oscillation Using Parallel Robot*, Journal of Military Science and Technology, No. 80, June 2022, pp. 156-67, doi:10.54939/1859-1043.j.mst.80.2022.156-167. (In Vietnamese)
[20] https://github.com/LINK-SIC-2021-Bernat-Granstrom/ship-simulator.